PERGAMON

Mathematical and Computer Modelling 35 (2002) 87–99

MATHEMATICAL AND COMPUTER MODELLING

www.elsevier.com/locate/mcm

Numerical Scheme for Swift-Hohenberg Equation with Strict Implementation of Lyapunov Functional

C. I. CHRISTOV*
Department of Mathematics, University of Louisiana at Lafayette
Lafayette, LA 70504-1010, U.S.A.
christov@louisiana.edu

J. PONTES
Metallurgy and Materials Engineering Department/COPPE/UFRJ
P.O. Box 68505, 21945-970, Rio de Janeiro, R. J. Brazil

(Received January 2001; accepted May 2001)

Abstract—In this paper, we consider a nonlinear generalized diffusion equation called the Swift-Hohenberg equation (SH) for which a Lyapunov functional is known. We develop a computationally efficient second-order in time implicit difference scheme based on the operator-splitting method. Internal iterations are used to make the scheme both nonlinear and implicit. We prove that the scheme allows strict (independent of the truncation error) implementation of a discrete approximation of the Lyapunov functional. The new scheme is used to investigate the pattern formation from random initial conditions, and spatially chaotic states are found. © 2001 Elsevier Science Ltd. All rights reserved.

Keywords—Nonlinear systems, Lyapunov functional, Implicit finite difference schemes.

1. INTRODUCTION

A widely accepted model for the thermal convection in a thin layer of fluid heated from below is the so-called Swift-Hohenberg equation (SH, for brevity) [1], which is a nonlinear parabolic equation containing fourth-order space-derivatives (generalized diffusion equation). It describes the pattern formation in fluid layers confined between horizontal well-conducting boundaries.

Unlike the models that describe wave propagation on the surface of convective layer, the SH equation possesses a Lyapunov functional which ensures the potential behaviour of the solution. Among other properties of the potential evolution is that one cannot have spatio-temporal chaos, but only spatial ones. However, if one uses a difference scheme which does not faithfully represent the Lyapunov functional, one might encounter numerically some nonphysical effects. For instance, when the Lyapunov functional is only approximately enforced, then initially the solution approaches one of the attractors in the functional space, but eventually leaves the domain

*Author to whom all correspondence should be addressed.

The work of C. I. Christov is supported in part by Grant LEQSF (1999–2002)-RD-A-49 from the Louisiana Board of Regents. J. Pontes acknowledges financial support from CNPq (Brazil) through Grant No. 452399/00-9(NV). Part of the simulations were performed on the IBM RS-6000 of the NACAD-UFRJ Computer Center at the Federal University of Rio de Janeiro, Brazil.

PII: S0895-7177(01)00151-0

of attraction of that particular steady-state solution after being "kicked" from one of the small disturbances, the latter arising from the inadequate approximation. Then the solution may keep wandering between several of the attractors exhibiting spatio-temporal chaotic behavior, which is not possible for the original model.

Solving SH numerically is a challenge because of the interplay between the higher-order diffusion (higher-order spatial derivatives) and nonlinearity on one hand, and the presence of a Lyapunov functional on the other. A computationally efficient difference scheme for SH was developed in [2], where a first-order in time implicit time-stepping is used in the framework of the operator-splitting methods.

There are very few papers in the literature which deal with the problems connected to the numerical implementation of an additional integral constraint on the solution, such as the Lyapunov functional. For dissipative systems (Swift-Hohenberg or complex Landau-Ginzburg equation), an elucidating discussion can be found in [3,4]. For the case of Lyapunov constraint in a conservative system (such as nonlinear Schrödinger equation), one is referred to [5]. Though some fine approximations of the additional integral constraint are presented in the above mentioned papers, they are not, in fact, strictly preserving approximations. We believe the strict implementation is crucial if one is to deal with more complex models.

In the present work, a finite-difference semi-implicit coordinate-splitting scheme of second order in time and space is developed for SH equation subject to generalized Dirichlet boundary conditions. The proposed scheme employs internal iterations to secure adequate approximation of the nonlinear term. It is proved that the scheme strictly satisfies a discrete approximation of the Lyapunov functional.

2. POSING THE PROBLEM

Consider a rectangular region $D : \{x \in [0, L_x,], y \in [0, L_y]\}$ with boundary ∂D at which different types of b.c. can be imposed. Consider the following generalized diffusion equation (GDE):

$$\frac{\partial u}{\partial t} = -D\left(\Delta + \kappa^2\right)^2 + F(u) \equiv -D\Delta\Delta u - 2D\kappa^2\Delta u - D\kappa^4 + F(u). \tag{2.1}$$

For the cubic nonlinearity, one has the following potential function:

$$F(u) = -\frac{dU(u)}{du} = \varepsilon(x)u - gu^3, \qquad U(u) = -\frac{\varepsilon(x)}{2}u^2 + \frac{g}{4}u^4. \tag{2.2}$$

Equation (2.1), with (2.2) acknowledged, is the Swift-Hohenberg equation (SH, for brevity) derived for the Rayleigh-Bénard convection to account for the formation of convective rolls in high Prandtl number fluid layers. The variable $u(x, y, t)$ describes the horizontal planform of the temperature deviation from the conductive profile.

The correct set of lateral b.c. is the one which secures that the evolution of the "energy" $\int v^2$ depends only on its production or dissipation in the bulk, but not on the surface. In other words, in the balance equation for the evolution of energy,

$$\begin{aligned}\frac{d}{dt}\frac{1}{2}\int_D v^2\,\mathrm{d}x\,\mathrm{d}y = &-\oint_{\partial D} v\frac{\partial a_4(x,y,t)\Delta v}{\partial n}\,\mathrm{d}l - \oint_{\partial D} a_4(x,y,t)\Delta v\frac{\partial v}{\partial n}\,\mathrm{d}l \\ &-\oint_{\partial D} a_2(x,y,t)v\frac{\partial v}{\partial n}\,\mathrm{d}l - \int_D a_0(x,y,t)(\Delta v)^2\,\mathrm{d}x\,\mathrm{d}y \\ &-\int_D a_2(x,y,t)(\nabla v)^2\,\mathrm{d}x\,\mathrm{d}y - \int_D a_0(x,y,t)v^2\,\mathrm{d}x\,\mathrm{d}y,\end{aligned} \tag{2.3}$$

one has to make the surface integrals vanish. This can happen if one of the following admissible b.c. conditions are imposed:

$$v = \frac{\partial v}{\partial n} = 0, \quad v = \Delta v = 0, \quad \frac{\partial v}{\partial n} = \frac{\partial \Delta v}{\partial n} = 0, \qquad (x,y) \in \partial D, \tag{2.4}$$

where n stands for the outward normal direction to the boundary ∂D. We call $(2.4)_1$ and $(2.4)_2$ "generalized Dirichlet conditions" of the first and second kind, respectively. Condition $(2.4)_3$ involves only derivatives at the boundary, hence, the coinage "generalized Neumann condition".

The main feature of (2.1) is that the damping of perturbations occurs via the fourth-order spatial derivatives, while the term with second-order spatial derivatives enhances the perturbations. This allows the occurrence of a linear bifurcation of the solution for certain values of the parameters and/or the size of domain. The nontrivial solutions branch out from a (generally motionless) reference state. Their shapes are the result of the interplay between the complicated linear operator and the nonlinearity. From the perspective of GDE, it is clear that a bifurcation can take place only for sufficiently large domains whose size is commensurate with the length scales of the patterns.

SH admits a nonincreasing Lyapunov functional

$$\Psi = \int_D \left\{ -\frac{\varepsilon}{2}u^2 + \frac{g}{4}u^4 + \frac{D}{2}\left[(\Delta u)^2 - 2\kappa^2(\nabla u)^2 + \kappa^4 u^2\right] \right\} \mathrm{d}x\,\mathrm{d}y, \tag{2.5}$$

$$\frac{\partial \Psi}{\partial t} = -\int_D \left(\frac{\partial u}{\partial t}\right)^2 \mathrm{d}x\,\mathrm{d}y < 0, \tag{2.6}$$

which rules out the complex temporal or spatio-temporal behavior in the long time (turbulent, oscillatory, or chaotic) and allows formation of steady convective patterns. In their turn, these steady patterns can be quite complicated in shape, e.g., spatially chaotic.

Consider the rectangle $x \in [0, L_x]$, $y \in [0, L_y]$ and the Dirichlet b.c. of the first and second kind:

$$u = \frac{\partial u}{\partial x} = 0, \quad \text{for } x = 0,\ L_x; \qquad u = \frac{\partial u}{\partial y} = 0, \quad \text{for } y = 0,\ L_y, \tag{2.7}$$

$$u = \frac{\partial^2 u}{\partial x^2} = 0, \quad \text{for } x = 0,\ L_x; \qquad u = \frac{\partial^2 u}{\partial y^2} = 0, \quad \text{for } y = 0,\ L_y, \tag{2.8}$$

Respectively, the Neumann condition is

$$\frac{\partial u}{\partial x} = \frac{\partial^2 u}{\partial x^2} = 0, \quad \text{for } x = 0,\ L_x, \qquad \frac{\partial u}{\partial y} = \frac{\partial^2 u}{\partial y^2} = 0, \quad \text{for } y = 0,\ L_y, \tag{2.9}$$

There is no restriction to the use of mixed types of b.c. which are combinations of Dirichlet and Neumann conditions. If the scheme and algorithm perform properly for the "pure" cases (including the Neumann one), then they will do the same for the mixed cases, since any admissible (in the sense of (2.3) mixture of boundary conditions yields a well-posed boundary value problem. For the sake of simplicity, we restrict ourselves in the present work to Dirichlet conditions of the first kind.

3. DIFFERENCE SCHEME

3.1. Implicit Time-Stepping

It is not possible to achieve a strict satisfaction of a discrete version of the Lyapunov functional with an explicit scheme which has only two time stages (levels). On the other hand, it is not obvious how the problem can be solved through using multilevel scheme. It is *a priori* clear that a scheme which is both implicit in time and nonlinear will possess the necessary symmetry to accommodate for the existence of a nonincreasing functional. The key to the scheme which satisfies the additional integral constraint (the Lyapunov functional) is the approximation of the nonlinear potential term. A scheme for (2.1) which is implicit and nonlinear reads

$$\frac{u^{n+1} - u^n}{\tau} = D\left[-\frac{\partial^4}{\partial x^4} - \frac{\partial^4}{\partial y^4} - 2k^2\frac{\partial^2}{\partial x^2} - 2k^2\frac{\partial^2}{\partial y^2} - 2\frac{\partial^4}{\partial x^2 \partial y^2} - k^4\right]\frac{u^{n+1} + u^n}{2} - \frac{U\left(u^{n+1}\right) - U\left(u^n\right)}{u^{n+1} - u^n}, \tag{3.1}$$

where $U(u)$ stands for the potential of the nonlinear force acting upon the system. For the particular case of quartic potential, the nonlinear term adopts the form

$$-\frac{U\left(u^{n+1}\right)-U\left(u^{n}\right)}{u^{n+1}-u^{n}}=\frac{\varepsilon(x)}{2}\left[u^{n+1}+u^{n}\right]-\frac{g}{4}\left[\left(u^{n+1}\right)^{3}+\left(u^{n+1}\right)^{2}u^{n}+u^{n+1}\left(u^{n}\right)^{2}+\left(u^{n}\right)^{3}\right].$$

3.2. Internal Iterations

Scheme (3.1) is nonlinear and can be solved only by means of iterating the solution within a given time step. An additional benefit from the iterations is that they allow us to alleviate a possible problem connected with the inversion of the linear operators when they are not negative definite. This kind of complication can be expected only when $\max\{L_x, L_y\}k_0 \geq \alpha$, where α can be estimated from the inclusion theorem. As already mentioned, a simple consequence of the nondefiniteness of the linear operator is the occurrence of a linear bifurcation of the stationary problem. We tackle this complication by means of an explicit approximation of the second-order terms. Thus, the iterative scheme reads

$$\begin{aligned}\frac{u^{n,k+1}-u^{n}}{\tau}=&\left[-D\frac{\partial^{4}}{\partial x^{4}}-D\frac{\partial^{4}}{\partial y^{4}}-Dk^{4}+\varepsilon(x)\right]\frac{u^{n,k+1}+u^{n}}{2}\\&+\left[-2Dk^{2}\frac{\partial^{2}}{\partial x^{2}}-2Dk^{2}\frac{\partial^{2}}{\partial y^{2}}-2D\frac{\partial^{4}}{\partial x^{2}\partial y^{2}}\right]\frac{u^{n,k}+u^{n}}{2}\\&-\frac{g}{4}\left[\left(u^{n,k}\right)^{2}+u^{n,k}u^{n}+\left(u^{n}\right)^{2}\right]u^{n,k+1}-\frac{g}{4}\left(u^{n}\right)^{3}.\end{aligned}\tag{3.2}$$

Here the superscript $(n, k+1)$ designates the current ("new") iteration of the unknown set function, while the indices (n, k) and (n) distinguish the quantities known from the previous iteration and the previous time step, respectively. The scheme with internal iterations is linear for $u^{n,k+1}$. The internal iterations are conducted until the following criterion is satisfied:

$$\frac{\max\left\|u^{n,K+1}-u^{n,K}\right\|}{\max\left\|u^{n,K+1}\right\|}<\delta,\tag{3.3}$$

for certain $k = K$. Then the last iteration gives the sought function on the new time stage, $u^{n+1} \stackrel{\text{def}}{=} u^{n,K+1}$.

The gist of the concept of internal iterations is that the same time step is repeated until convergence. Since the iterative process begins from an initial condition which is the value of the sought function from the previous time step, the number of internal iterations needed for convergence depends heavily on the magnitude of the time increment τ. For smaller τ, the initial condition for the iterations is closer to the sought function and the number of iterations is expected to be small. The trade-off is that a very small τ requires a larger number of time steps which increases the overall number of arithmetic operations per nodal point. Conversely, an inappropriately large τ will bring about a larger number of internal iterations per time step, increasing significantly the computational time needed to achieve a single time step, thus dispelling the advantage of the larger "strides" (the faster time-stepping). The dependence of the number of internal iterations on τ is nonlinear and leaves room for optimization. Our numerical experiments show that the calculations are cost effective if the number of internal iterations is in the interval $4 \leq K \leq 16$. This estimate calls for a reduction of the time step when faster processes are treated for which the evolution from a given time stage to the next time stage involves a significant deformation of the field. This means that when faster temporal transients are involved, the usage of larger time steps τ leading to $K \gg 20$ is not justified regardless of the fact that, formally speaking, the implicit scheme is still stable.

3.3. The Splitting

The inversion of the matrix of equation (3.2) is a rather costly procedure even though it is sparse. The 3D case is drastically more expensive. Moreover, the internal iterations require the process to be repeated several times during each time step. Then it is only natural to introduce operator splitting in order to minimize the operations per unit iteration, and hence, per one time step.

We settle here for the *second Douglas scheme* [6] (also called "scheme of stabilizing correction" [7]), which gives the full-time-step approximation for noncommutative operators and is more robust for nonlinear problems than ADI (see, [7] for a review of the splitting schemes and strategies). Another advantage of the stabilizing correction is that for linear problems in 3D, it is absolutely stable, while ADI is not. We generalize the Douglas scheme for fourth-order operators and modify it to be second-order accurate in time (a Crank-Nicolson type of scheme) as follows:

$$\begin{aligned}\frac{\tilde{u}-u^n}{\tau} &= L_{11}^{n,k}\tilde{u} + L_{22}^{n,k}u^n + \frac{1}{2}\left[-D\frac{\partial^4}{\partial x^4} - D\frac{\partial^4}{\partial y^4} - Dk^4 + \varepsilon(x) + \frac{g}{2}(u^n)^2\right]u^n \\ &\quad + \frac{1}{2}\left[-L_{12} - L_1 - L_2\right]\left[u^{n,k} + u^n\right], \\ \frac{u^{n,k+1}-\tilde{u}}{\tau} &= L_2^{n,k}\left(u^{n,k+1} - u^n\right),\end{aligned} \tag{3.4}$$

where

$$L_{11}^{n,k} \stackrel{\text{def}}{=} -\frac{D}{2}\frac{\partial^4}{\partial x^4} - \frac{D}{4}k^4 + \frac{g}{8}\left[\left(u^{n,k}\right)^2 + u^{n,k}u^n + (u^n)^2\right] + \frac{\varepsilon(x)}{2},$$

$$L_{22}^{n,k} \stackrel{\text{def}}{=} -\frac{D}{2}\frac{\partial^4}{\partial y^4} - \frac{D}{4}k^4 + \frac{g}{8}\left[\left(u^{n,k}\right)^2 + u^{n,k}u^n + (u^n)^2\right] + \frac{\varepsilon(x)}{2}, \tag{3.5}$$

$$L_{12} \stackrel{\text{def}}{=} 2D\frac{\partial^4}{\partial x^2 \partial y^2}, \qquad L_1 \stackrel{\text{def}}{=} 2Dk^2\frac{\partial^2}{\partial x^2}, \qquad L_2 \stackrel{\text{def}}{=} 2Dk^2\frac{\partial^2}{\partial y^2}. \tag{3.6}$$

In order to show that the splitting scheme approximates the original implicit scheme, we rewrite (3.4) as follows:

$$\begin{aligned}\left[E - \tau L_{11}^{n,k}\right]\tilde{u} &= \left[E + \tau L_{22}^{n,k}\right]u^n + \frac{\tau}{2}\left[-L_{12} - L_1 - L_2\right]\left[u^{n,k} + u^n\right] \\ &\quad + \frac{\tau}{2}\left[-\frac{\partial^4}{\partial x^4} - \frac{\partial^4}{\partial y^4} - k^4 + \varepsilon(x) + \frac{g}{2}(u^n)^2\right]u^n, \\ \left[E - \tau L_{22}^{n,k}\right]u^{n,k+1} &= \tilde{u} - \tau L_{22}^{n,k}u^n.\end{aligned} \tag{3.7}$$

Now we are prepared to eliminate the intermediate variable $\tilde{u}$. This is done after applying the operator $[E - \tau L_{11}^{n,k}]$ to the second of equations (3.7) and adding the result to the first one, namely,

$$\begin{aligned}\left[E - \tau L_{11}^{n,k}\right]\left[E - \tau L_{22}^{n,k}\right]u^{n,k+1} &= \left[E + \tau L_{22}^{n,k}\right]u^n - \tau\left[E - \tau L_{11}^{n,k}\right]L_{22}^{n,k}u^n \\ &\quad + \frac{\tau}{2}\left[-L_{12} - L_1 - L_2\right]\left[u^{n,k} + u^n\right] + \frac{\tau}{2}\left[-\frac{\partial^4}{\partial x^4} - \frac{\partial^4}{\partial y^4} - k^4 + \varepsilon(x) + \frac{g}{2}(u^n)^2\right]u^n,\end{aligned}$$

or else,

$$\begin{aligned}\left[E + \tau^2 L_{11}^{n,k}L_{22}^{n,k}\right]\frac{u^{n,k+1} - u^n}{\tau} &= \left(L_{11}^{n,k} + L_{22}^{n,k}\right)u^{n,k+1} + \frac{1}{2}\left[-L_{12} - L_1 - L_2\right]\left[u^{n,k} + u^n\right] \\ &\quad + \frac{1}{2}\left[-D\frac{\partial^4}{\partial x^4} - D\frac{\partial^4}{\partial y^4} - Dk^4 + \varepsilon(x) + \frac{g}{2}(u^n)^2\right]u^n.\end{aligned} \tag{3.8}$$

Upon acknowledging (3.5),(3.6), it is readily shown that (3.8) is, in fact, (3.2) save the *positive definite* operator of norm larger than unity

$$B \equiv E + \tau^2 L_{11}^{n,k} L_{22}^{n,k} = E + O\left(\tau^2\right), \tag{3.9}$$

acting upon the time difference $(u^{n+1} - u^n)/\tau$. Acting upon the time difference means that the operator B has no influence on the steady-state result. The fact that $\|B\| > 1$ means that the splitting scheme is more stable than the original implicit scheme. The splitting scheme approximates the desired scheme in full-time steps within the adopted order of approximation $O(\tau^2)$. Thus, employing a splitting does not degrade the temporal approximation of the scheme. In other words, the splitting scheme coincides with the original scheme within the order of approximation of the latter.

3.4. Spatial Discretization

Consider a staggered mesh in both spatial directions, namely,

$$x_i = -\frac{h_x}{2} + (i-1)\, h_x, \quad h_x \equiv \frac{L_x}{M-2}, \qquad y_i = -\frac{h_y}{2} + (j-1)\, h_y, \quad h_y \equiv \frac{L_y}{N-2},$$

where M, N are the number of points in x- and y-directions, respectively. Let $\Phi_{i,j}$ be an arbitrary set function defined on the above described mesh. We confine ourselves to the case of constant coefficients. Then the simplest symmetric difference approximations of the differential operators read

$$\begin{aligned}
\Lambda_{11}\Phi_{i,j} &= -D\frac{\Phi_{i+2,j} - 4\Phi_{i+1,j} + 6\Phi i,j - 4\Phi_{i-1,j} + \Phi_{i-2,j}}{h_x^4} \approx -D\frac{\partial^4\Phi}{\partial x^4} \stackrel{\text{def}}{=} L_{11}\Phi, \\
\Lambda_{22}\Phi_{i,j} &= -D\frac{\Phi_{i,j+2} - 4\Phi_{i,j+1} + 6\Phi i,j - 4\Phi_{i,j-1} + \Phi_{i,j-2}}{h_y^4} \approx -D\frac{\partial^4\Phi}{\partial y^4} \stackrel{\text{def}}{=} L_{22}\Phi, \\
\Lambda_{12}\Phi_{i,j} &= -\frac{D}{h_x^2 h_y^2}\left[\Phi_{i+1,j+1} - 2\Phi_{i+1,j} + \Phi_{i+1,j-1} - 2(\Phi_{i,j+1} - 2\Phi_{i,j} + \Phi_{i,j-1})\right. \\
&\quad \left. + \Phi_{i+1,j+1} - 2\Phi_{i+1,j} + \Phi_{i+1,j-1}\right] \approx -D\frac{\partial^4\Phi}{\partial x^2 \partial y^2} \stackrel{\text{def}}{=} L_{12}\Phi, \\
\Lambda_{xx}\Phi_{i,j} &= 2Dk^2\frac{\Phi_{i+1,j} - 2\Phi_{i,j} + \Phi_{i-1,j}}{h_x^2} \approx 2Dk^2\frac{\partial^2\Phi}{\partial x^2} \stackrel{\text{def}}{=} L_2\Phi, \\
\Lambda_{yy}\Phi_{i,j} &= 2Dk^2\frac{\Phi_{i,j+1} - 2\Phi_{i,j} + \Phi_{i,j-1}}{h_x^2} \approx 2Dk^2\frac{\partial^2\Phi}{\partial y^2} \stackrel{\text{def}}{=} L_1\Phi.
\end{aligned} \tag{3.10}$$

Here, the notation Λ stands for the discrete approximation of the respective operator L.

On the staggered mesh, all kinds of b.c. are easily approximated with second-order approximation, namely,

$$\begin{aligned}
&u_{1,j} + u_{2,j} \approx 2u\,\big|_{x=0}, && u_{3,j} - u_{2,j} - u_{1,j} + u_{0,j} \approx 2h_x^2\frac{\partial^2 u}{\partial x^2}\bigg|_{x=0}, \\
&u_{M,j} - u_{M-1,j} \approx h_x\,\frac{\partial u}{\partial x}\bigg|_{x=L_x}, && u_{3j} - 3u_{2j} + 3u_{1j} + u_{0j} \approx 6h_x^3\frac{\partial^3 u}{\partial x^3}\bigg|_{x=0}, \\
&u_{M-1,j} + u_{M,j} \approx 2u\,\big|_{x=L_x}, && u_{M+1,j} - u_{M,j} - u_{M-1,j} + u_{M-2,j} \approx 2h_x^2\frac{\partial^2 u}{\partial x^2}\bigg|_{x=L_x}, \\
&u_{2,j} - u_{1,j} \approx h_x\,\frac{\partial u}{\partial x}\bigg|_{x=0}, && u_{M+1,j} - 3u_{M,j} + 3u_{M-1,j} + u_{M-2,j} \approx 6h_x^3\frac{\partial^3 u}{\partial x^3}\bigg|_{x=L_x},
\end{aligned} \tag{3.11}$$

for $j = 3, \ldots, N-2$,

and

$$
\begin{aligned}
&u_{i,1}+u_{i,2}\approx 2u\left.\right|_{y=0}, && u_{i,3}-u_{i,2}-u_{i,1}+u_{i,0}\approx 2h_y^2\left.\frac{\partial^2 u}{\partial y^2}\right|_{y=0},\\
&u_{i,2}-u_{i,1}\approx h_y\left.\frac{\partial u}{\partial y}\right|_{y=0}, && u_{i,3}-3u_{i,2}+3u_{i,1}+u_{i,0}\approx 6h_y^3\left.\frac{\partial^3 u}{\partial y^3}\right|_{y=0},\\
&u_{i,N-1}+u_{i,N}\approx 2u|_{x=L_y}, && u_{i,N+1}-u_{i,N}-u_{i,N-1}+u_{i,N-2}\approx 2h_y^2\left.\frac{\partial^2 u}{\partial y^2}\right|_{y=L_y},\\
&u_{i,N}-u_{i,N-1}\approx h_y\left.\frac{\partial u}{\partial y}\right|_{y=L_y}, && u_{i,N+1}-3u_{i,N}+3u_{i,N-1}+u_{i,N-2}\approx 6h_y^3\left.\frac{\partial^3 u}{\partial y^3}\right|_{y=L_y},
\end{aligned}
\tag{3.12}
$$

for $i=3,\dots,N-2$.

Hence, the approximations of the Dirichlet b.c. of the first kind read

$$
\begin{aligned}
u_{1j}&=u_{2j}=0, & u_{Mj}&=u_{M-1j}=0,\\
u_{i1}&=u_{i2}=0, & u_{iN}&=u_{iN-1}=0.
\end{aligned}
\tag{3.13}
$$

4. IMPLEMENTATION OF THE LYAPUNOV FUNCTIONAL

After the iterations converge, one has $u^{n+1}=u^{n,k+1}=u^{n,k}$, and hence, one arrives at a nonlinear scheme in full-time steps which is exactly the difference approximation of scheme (3.1) when, in the latter, the operators L are replaced by Λ, namely,

$$
\frac{u^{n+1}-u^n}{\tau}=(\Lambda_{11}+\Lambda_{22}-\Lambda_1-\Lambda_2+2\Lambda_{12})\frac{u^{n+1}+u^n}{2}-\frac{U\left(u^{n+1}\right)-U\left(u^n\right)}{u^{n+1}-u^n},
\tag{4.1}
$$

where

$$
\frac{U\left(u^{n+1}\right)-U\left(u^n\right)}{u^{n+1}-u^n}=-\frac{\varepsilon}{2}\left[u^{n+1}+u^n\right]+\frac{g}{4}\left[\left(u^{n+1}\right)^3+\left(u^{n+1}\right)^2u^n+u^{n+1}\left(u^n\right)^2+\left(u^n\right)^3\right].
$$

Note that in the left-hand side, we neglected the $O(\tau^2)$ contribution to the operator B from (3.9) as asymptotically vanishing with respect to unity.

Upon multiplying equation (4.1) by $(u_{ij}^{n+1}-u_{ij}^n)/\tau$ and taking the sum over the spatial indices, one obtains

$$
\begin{aligned}
\sum_{i=2}^{M-1}\sum_{j=2}^{N-1}\left[\frac{u_{i,j}^{n+1}-u_{i,j}^n}{\tau}\right]^2&=\sum_{i=2}^{M-1}\sum_{j=2}^{N-1}\left\{\frac{\varepsilon}{2\tau}\left[\left(u_{i,j}^{n+1}\right)^2-\left(u_{i,j}^n\right)^2\right]-\frac{g}{4\tau}\left[\left(u_{i,j}^{n+1}\right)^4-\left(u_{i,j}^n\right)^4\right]\right\}\\
&+\sum_{i=2}^{M-1}\sum_{j=2}^{N-1}\frac{u_{i,j}^{n+1}-u_{i,j}^n}{\tau}\left[\Lambda_{11}+\Lambda_{22}-\Lambda_1-\Lambda_2+2\Lambda_{12}\right]\frac{u_{i,j}^{n+1}+u_{i,j}^n}{2}.
\end{aligned}
\tag{4.2}
$$

The last term is manipulated using integration (summation) by parts and the boundary conditions for u (3.11),(3.12) are acknowledged. We demonstrate the procedure on the difference operators in x-direction, and for Λ_{11}, we get

$$
\begin{aligned}
\frac{1}{2\tau}\sum_{i=2}^{M-1}u_{ij}^{n+1}\Lambda_{11}u_{i,j}^{n+1}&\stackrel{\text{def}}{=}-\frac{D}{2h_x^4\tau}\sum_{i=2}^{M-1}u_{ij}^{n+1}\left[u_{i-2,j}^{n+1}-4u_{i-1,j}^{n+1}+6u_{i,j}^{n+1}-4u_{i+1,j}^{n+1}+u_{i+2,j}^{n+1}\right]\\
&\equiv-\frac{D}{2h_x^4\tau}\sum_{i=3}^{M-2}u_{ij}^{n+1}\left[u_{i-2,j}^{n+1}-4u_{i-1,j}^{n+1}+6u_{i,j}^{n+1}-4u_{i+1,j}^{n+1}+u_{i+2,j}^{n+1}\right]
\end{aligned}
\tag{4.3}
$$

$$
\begin{aligned}
&= -\frac{D}{2h_x^4\tau}\sum_{i=2}^{M-1}\left[2u_{i+1,j}^{n+1}u_{i-1,j}^{n+1} - 4u_{i-1,j}^{n+1}u_{i,j}^{n+1} + 6u_{i,j}^{n+1}u_{i,j}^{n+1} - 4u_{i+1,j}^{n+1}u_{i,j}^{n+1}\right]\\
&\quad - \frac{D}{2h_x^4\tau}\left[-u_{Mj}^{n+1}u_{M-2j}^{n+1} - u_{M-1j}^{n+1}u_{M-3j}^{n+1} - u_{4j}^{n+1}u_{2j}^{n+1} - u_{3j}^{n+1}u_{1j}^{n+1}\right]\\
&\quad - \frac{D}{2h_x^4\tau}\left[4u_{Mj}^{n+1}u_{M-1j}^{n+1} + 4u_{M-1j}^{n+1}u_{M-2j}^{n+1} + 4u_{3j}^{n+1}u_{2j}^{n+1} + 4u_{2j}^{n+1}u_{1j}^{n+1}\right] \qquad (4.3(\text{cont.}))\\
&\quad - \frac{D}{2h_x^4\tau}\left[-6\left(u_{M-1j}^{n+1}\right)^2 - 6\left(u_{2j}^{n+1}\right)^2\right]\\
&= -\frac{D}{2\tau}\sum_{i=2}^{M-1}\left[\frac{u_{i+1,j}^{n+1} - 2u_{i,j}^{n+1} + u_{i-1,j}^{n+1}}{h_x^2}\right]^2.
\end{aligned}
$$

Similarly, for Λ_1,

$$
\begin{aligned}
-\frac{1}{2\tau}\sum_{i=2}^{M-1} u_{ij}^{n+1}\Lambda_1 u_{i,j}^{n+1} &\stackrel{\text{def}}{=} -\frac{2Dk^2}{2h_x^2\tau}\sum_{i=2}^{M-1} u_{ij}^{n+1}\left[u_{i-1,j}^{n+1} - 2u_{i,j}^{n+1} + u_{i+1,j}^{n+1}\right]\\
&= -\frac{2Dk^2}{2h_x^2\tau}\left\{\sum_{i=2}^{M-1}\left[u_{i,j}^{n+1}u_{i+1,j}^{n+1} - \frac{1}{2}\left(u_{i+1,j}^{n+1}\right)^2 - \frac{1}{2}\left(u_{i,j}^{n+1}\right)^2\right] + \frac{1}{2}\left[\left(u_2^{n+1}j\right)^2 - \left(u_{Mj}^{n+1}\right)^2\right]\right\}\\
&\quad - \frac{2Dk^2}{2h_x^2\tau}\left\{\sum_{i=2}^{M-1}\left[u_{ij}^{n+1}u_{i-1,j}^{n+1} - \frac{1}{2}\left(u_{i,j}^{n+1}\right)^2 - \frac{1}{2}\left(u_{i-1,j}^{n+1}\right)^2\right] - \frac{1}{2}\left[\left(u_1^{n+1}j\right)^2 + \left(u_{M-1j}^{n+1}\right)^2\right]\right\} \qquad (4.4)\\
&= \frac{2Dk^2}{4\tau}\sum_{i=2}^{M-1}\left\{\left[\frac{u_{i+1,j}^{n+1} - u_{i,j}^{n+1}}{h_x}\right]^2 + \left[\frac{u_{i,j}^{n+1} - u_{i-1,j}^{n+1}}{h_x}\right]^2\right\}.
\end{aligned}
$$

Making use of the same technique, one can show that

$$
\frac{1}{2\tau}\sum_{i=2}^{M-1} u_{ij}^{n}\Lambda_{11}u_{i,j}^{n+1} - u_{ij}^{n+1}\Lambda_{11}u_{i,j}^{n} = 0, \qquad \frac{1}{2\tau}\sum_{j=2}^{N-1} u_{ij}^{n}\Lambda_{22}u_{i,j}^{n+1} - u_{ij}^{n+1}\Lambda_{22}u_{i,j}^{n} = 0,
$$

$$
\frac{1}{2\tau}\sum_{i=2}^{M-1} u_{ij}^{n}\Lambda_{1}u_{i,j}^{n+1} - u_{ij}^{n+1}\Lambda_{1}u_{i,j}^{n} = 0, \qquad \frac{1}{2\tau}\sum_{j=2}^{N-1} u_{ij}^{n}\Lambda_{2}u_{i,j}^{n+1} - u_{ij}^{n+1}\Lambda_{2}u_{i,j}^{n} = 0.
$$

The terms connected with the y spatial derivative are treated in the same vein. The approximation of the mixed fourth derivative make use of the above derivations in both x- and y-direction. For the sake of convenience, we denote

$$
\Phi_{ij} = \frac{u_{i,j-1} - 2u_{ij} + u_{ij+1}}{h_y^2}.
$$

Then

$$
\begin{aligned}
\sum_{i=2}^{M-1} u_{ij}\frac{\Phi_{i-1,j} - 2\Phi_{ij} + \Phi_{i+1j}}{h_x^2} &= \sum_{i=2}^{M-1}\Phi_{ij}\frac{u_{i-1,j} - 2u_{ij} + u_{i+1j}}{h_x^2}\\
&\quad + \frac{u_{M-1j}\Phi_{Mj} - u_{1j}\Phi_{2j}}{h_x^2} + \frac{u_{Mj}\Phi_{M-1j} - u_{2j}\Phi_{1j}}{h_x^2}\\
&\equiv \sum_{i=2}^{M-1}\Phi_{ij}\frac{u_{i-1,j} - 2u_{ij} + u_{i+1j}}{h_x^2},
\end{aligned}
$$

and hence,

$$2\sum_{i=2}^{M-1}\sum_{j=2}^{N-1} u_{ij}\Lambda_{12}u_{ij} = 2\sum_{i=2}^{M-1}\sum_{j=2}^{N-1} \frac{u_{i-1,j}-2u_{ij}+u_{i+1j}}{h_x^2}\cdot\frac{u_{i,j-1}-2u_{ij}+u_{ij+1}}{h_y^2}.$$

Now it is readily shown that the right-hand side of (4.2) is the time difference of the Lyapunov functional Ψ,

$$\begin{aligned}
\frac{\Psi^{n+1}-\Psi^{n}}{\tau} &= -\sum_{i=2}^{M-1}\sum_{j=2}^{N-1}\left(\frac{u_{i,j}^{n+1}-u_{i,j}^{n}}{\tau}\right)^2 \\
\Psi^n &= \sum_{i=2}^{M-1}\sum_{j=2}^{N-1}\left[-\frac{\varepsilon}{2}\left(u_{i,j}^n\right)^2+\frac{g}{4}\left(u_{i,j}^n\right)^4+\frac{Dk^4}{2}\left(u_{i,j}^n\right)^2\right] \\
&\quad -\frac{2Dk^2}{4}\sum_{i=2}^{M-1}\sum_{j=2}^{N-1}\left\{\left[\frac{u_{i+1,j}^n-u_{i,j}^n}{h_x}\right]^2+\left[\frac{u_{i,j}^n-u_{i-1,j}^n}{h_x}\right]^2\right. \\
&\quad \left.+\left[\frac{u_{i,j+1}^n-u_{i,j}^n}{h_y}\right]^2+\left[\frac{u_{i,j}^n-u_{i,j-1}^n}{h_y}\right]^2\right\} \\
&\quad +\frac{D}{2}\sum_{i=2}^{M-1}\sum_{j=2}^{N-1}\left[\frac{u_{i+1,j}^n-2u_{i,j}^n+u_{i-1,j}^n}{h_x^2}+\frac{u_{i,j+1}^n-2u_{i,j}^n+u_{i,j-1}^n}{h_y^2}\right]^2.
\end{aligned} \tag{4.5}$$

The last formula presents an $O(\tau^2+h_x^2+h_y^2)$ approximation to the original Lyapunov functional (2.6) for the differential equation. The important point about a difference version of the Lyapunov functional (4.5) is that it is strictly enforced provided that the internal iterations converge. Its satisfaction does not depend on the truncation error.

5. NUMERICAL RESULTS

The main subject of the present work is to demonstrate the impact of the implementation of the Lyapunov functional on the numerical dynamics. As a featuring example, we consider a uniformly loaded (nonramped) system. From the point of view of dynamical systems, the behavior of the solution is essentially the same as of the ramped system [2], and the only differences are connected with the fact that larger number of solutions with different symmetries can take place for the uniformly loaded system.

First, we should mention that we checked the spatial and temporal discretizations on a simple case when the whole domain of the flow is occupied by a single convective cell. All mandatory tests involving doubling the temporal and spatial resolutions confirmed the second-order approximation of the scheme and the discrete implementation of the Lyapunov functional. The convergence of the internal iterations is tested for different values of the tolerance δ defined in equation (3.3). The quantitative differences between the patterns are negligible for $\delta \leq 10^{-5}$. This allows us to choose $\delta = 10^{-6}$.

Further on, we consider a situation with nontrivial pattern evolution. In order not to overload the presentation with too many complicated patterns, we consider a uniformly forced system of relatively small size $L_x = 10$ and $L_y = 10$ (referred to in what follows as 10×10 case). We chose large enough bifurcation (forcing) parameter $\varepsilon = 1$, which ensures that the system dynamics is nontrivial. The small system size keeps the required computational resources within the reasonable limit, while the relatively large bifurcation parameter secures that the flow regime becomes spatially chaotic.

For the sake of definiteness and backward compatibility with the works from the literature, we select $\kappa_0 = 3.1172$, $g = 12.9$, and $D = 0.015$ which values correspond to a typical Rayleigh-Bénard convection with pattern formation (see, e.g. [1]). When the size of the box is $L_x = L_y = 10$, the selected value for k_0 allows roughly nine convective cells in each direction. A staggered mesh with 82×82 points is used, which gives a spatial resolution of approximately ten points per convective cell.

The random initial condition is constructed by means of a random generator. The value of u in the first point (lower-left corner) is calculated with the random generator for a given initial seed and then the rest if the grid points are filled row-wise using the previous point as a seed for the next point. Finally, the initial field is renormalized to $[-1, 1]$. Thus, the pattern can be referred by the number of the initial seed.

The time evolution of the pattern is presented in Figure 1.

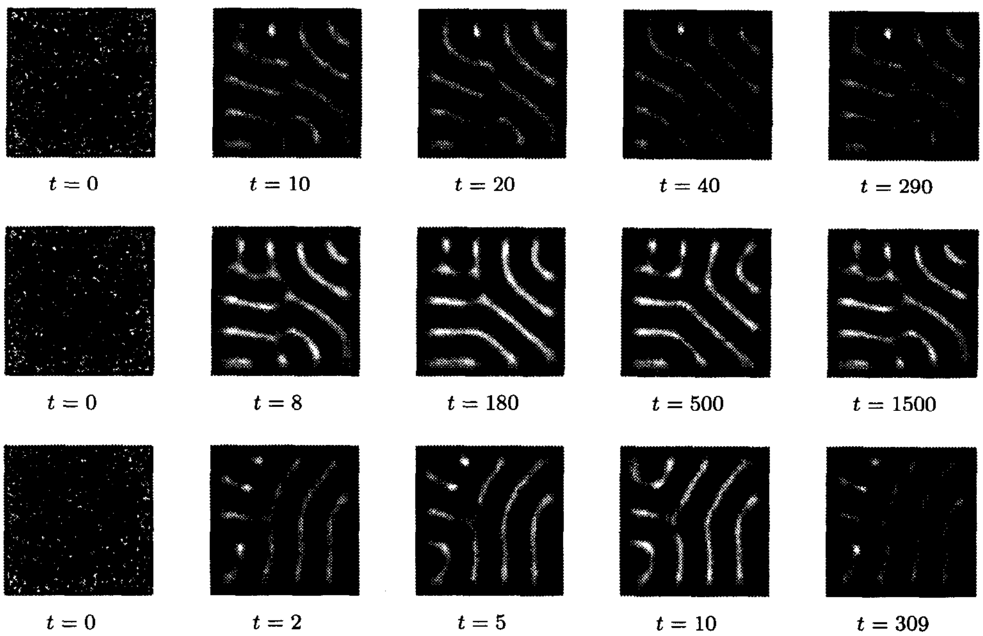

Figure 1. Top row: initial condition seed 34512, $\tau = 0.04$. Middle row: initial condition seed 34512, $\tau = 0.2$. Bottom row: initial condition seed 23456, $\tau = 0.04$.

The two upper rows of panels in Figure 1 are obtained with the same initial condition (seed 34512), but with different time increments $\tau = 0.04$ (the top row of panels) and $\tau = 0.2$ (the middle row). The lowest row presents the evolution for $\tau = 0.04$ when the calculations begin from a different initial condition (seed 23456). We have performed calculations with different time increments and for $\tau \leq 0.04$, and the results are graphically indistinguishable. The results show significant dependence on the time increment (in the sense that the final stationary pattern is qualitatively different) only for $\tau \geq 0.1$. Clearly, due to the truncation error of scheme, the two different time increments present two different routes to two different stationary solutions (compare the last two panels in the upper two rows of Figure 1). Still another stationary solution is reached when starting from the initial condition with seed 23456 (the lower row of panels in Figure 1).

We assess the rate of evolution of the pattern during the simulation by monitoring the relative L_1 norm defined as

$$L_1 = \frac{1}{\tau} \frac{\sum_{i,j} |u_{i,j}^{n+1} - u_{i,j}^{n}|}{\sum_{i,j} |u^{n+1}|}, \tag{5.1}$$

which roughly corresponds to the ratio between the spatial average of the modulus of time derivative u_t and the spatial average of the modulus of the function itself.

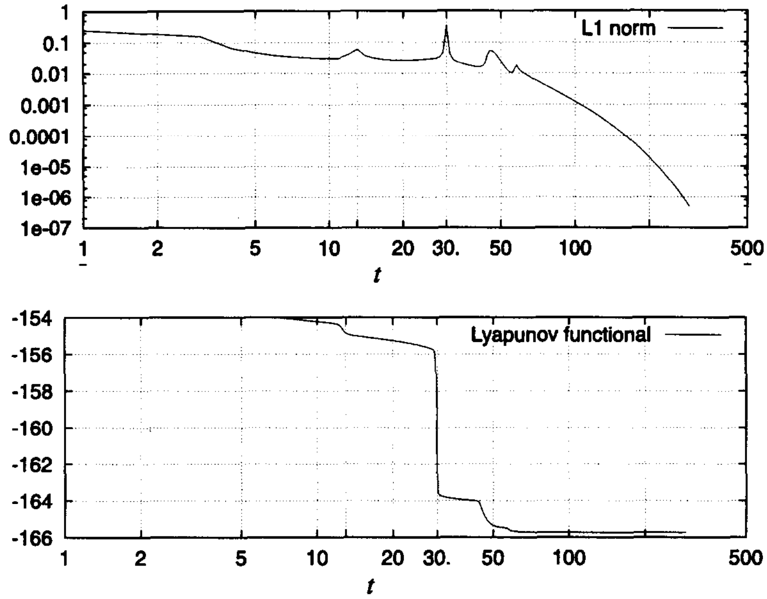

Figure 2. Seed 34512: $L_1(t)$ (upper panel) and $\Psi(t)$ (lower panel) curves for $\tau = 0.04$.

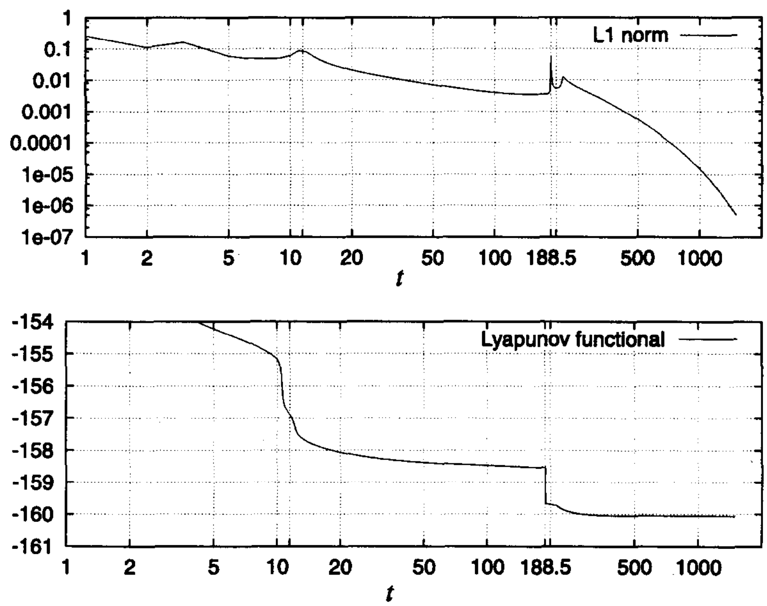

Figure 3. Seed 34512: $L_1(t)$ (upper panel) and $\Psi(t)$ (lower panel) curves for $\tau = 0.2$.

The calculations began from a random initial condition and proceeded until $L_1 \leq 5 \times 10^{-7}$, when it can be assumed that the motion is virtually steady.

Let us begin with the first case in Figure 1. Initially, the system displays a focus near the bottom of the domain. For times between $20 \leq t \leq 40$, it abruptly disappears provoking a precipitation of the value of the Lyapunov functional $\Psi(t)$ (lower panel of Figure 2). The evolution of the pattern accelerates at this moment, as precisely captured by the sudden increase of the norm $L_1(t)$ (upper panel of Figure 2).

We also monitored the number of internal iterations. In the time intervals of slow evolution, the number of internal iterations is around two to three. As expected, this number increases in the time intervals of rapid evolution (the same intervals in which the L_1 norm increases). For instance, in the first case, the number of iterations is two for $t > 10$ and increases to four

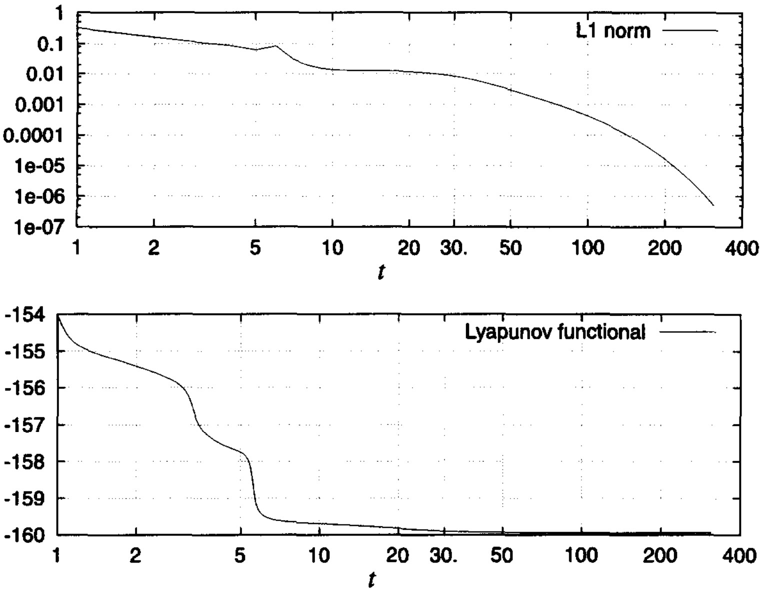

Figure 4. Seed 23456: $L_1(t)$ (upper panel) and $\Psi(t)$ (lower panel) curves for $\tau = 0.04$.

around $t \approx 29.6$. The second case begins with ten iterations and near $T = 180$, their number decreases down to four and goes up again to eight iterations in the region of fastest evolution, $t \approx 188.65$. The number of iterations in this case is larger than for the previous case because the time increment $\tau = 0.2$ is five times larger, which automatically requires a larger number of internal iterations.

As already mentioned above, the bifurcation nature of the problem shows up when a relatively large time increment is chosen $\tau = 0.2$ and the evolution takes a rather different path in the phase space, ending up in another stationary pattern. The evolution of L_1 and Ψ in this case are presented in Figure 3. Once again the streamlining and simplification of the pattern are connected with sharp precipitations in the Lyapunov functional.

As a third example, we present the evolution of the pattern beginning from a different initial condition. Figure 4 shows the L_1-norm and the Lyapunov functional as functions of time t. The quantitative behavior is similar to the previous two cases, but the stationary pattern is different. In addition, the fronts in L_1 and Ψ are not as steep in this case. Respectively, the number of iterations is three for $1 \leq t \leq 5$ and increase just to four for $t \approx 5.5$ (when the changes take place in this case).

Manipulating the initial condition, we succeeded in obtaining a plethora of solutions. It goes beyond the framework of the present paper to present an exhaustive study of the different end-stage chaotic steady states.

6. CONCLUSIONS

In the present work, we have created an operator-splitting difference scheme for the numerical solution of nonlinear diffusion equations containing fourth-order space-derivatives. The scheme is of second-order approximation both in time and space and does not contain artificial dispersion, hence, the disturbances are quickly attenuated. It is fully implicit, owing to the use of internal iterations. The main characteristic of the scheme is that a discrete version of the Lyapunov functional which holds for the original differential equation is strictly implemented.

The performance of the scheme is demonstrated for the evolution of the solution of the Swift-Hohenberg (SH) equation. The latter models the Rayleigh-Bénard convection in a horizontal layer. As a featuring example, we treat a domain of moderate size (10×10), but with relatively large value of the loading parameter which triggers the bifurcation of a plethora of different regimes. We present here three different cases of temporal evolution from a random initial condition. The strict implementation of the Lyapunov functional with its nonincreasing behaviour is clearly demonstrated. The numerically obtained Lyapunov functional decreases more rapidly when the pattern undergoes qualitative changes (when the solution enters the immediate vicinity of the respective attractor). In all cases, the evolution ended up in a spatially chaotic pattern. No temporal chaos was possible due to the strict satisfaction of the Lyapunov functional.

The proposed difference scheme can serve as a model for constructing approximations to nonlinear physical system when additional constraints, such as the Lyapunov functional, are imposed on the solution.

REFERENCES

1. J. Swift and P.C. Hohenberg, Hydrodynamic fluctuations at the convective instability, *Phys. Rev. A* **15**, 319–328 (1977).
2. C.I. Christov, J. Pontes, D. Walgraef and M.G. Velarde, Implicit time splitting for fourth-order parabolic equations, *Comp. Meth. Appl. Mech. & Eng.* **148**, 209–224 (1997).
3. J. Viñals, E. Hernandez García, M. San Miguel and R. Toral, Numerical study of the dynamic aspects of pattern selection in the stochastic Swift-Hohenberg equation in one dimension, *Phys. Rev. A* **44**, 1123-1133 (1991).
4. R. Montagne, E. Hernandez-García and M. San Miguel, Numerical study of a Lyapunov functional for the complex Ginzburg-Landau equation, *Physica D* **96**, 47-65 (1996).
5. I.A. Ivonin, V.P. Pavlenko and H. Persson, Self-consistent turbulence in the two-dimensional nonlinear Schrodinger equation with a repulsive potential, *Phys. Rev. E* **60**, 492-499 (1999).
6. J. Douglas and H.H. Rachford, On the numerical solution of heat conduction problems in two and three space variables, *Trans. Amer. Math. Soc.* **82**, 421–439 (1956).
7. N.N. Yanenko, *Method of Fractional Steps*, Gordon and Breach, New York, (1971).